Available online at www.sciencedirect.com
ScienceDirect
Applied Catalysis B: Environmental 82 (2008) 27–36
APPLIED CATALYSIS B: ENVIRONMENTAL
www.elsevier.com/locate/apcatb

Kinetics of the photocatalytic disinfection of *Escherichia coli* suspensions

Javier Marugán, Rafael van Grieken *, Carlos Sordo, Cristina Cruz

Department of Chemical and Environmental Technology, ESCET, Universidad Rey Juan Carlos, C/Tulipán s/n, 28933 Móstoles, Madrid, Spain

Received 13 November 2007; received in revised form 23 December 2007; accepted 2 January 2008
Available online 15 January 2008

Abstract

The photocatalytic inactivation of *Escherichia coli* suspensions has been successfully modelled with kinetic equations based on a simplified reaction mechanism using three parameters: kinetic constant (k), pseudo-adsorption constant (K) and inhibition coefficient (n). This model has been used to fit complex bacterial inactivation curves with shoulders and tails regions in addition to the classical log-linear behaviour. Experiments performed with increasing concentrations of titania, using TiO_2/SiO_2 photocatalysts and waters with different composition indicates that the most sensitive parameters are the kinetic and the pseudo-adsorption constant, whereas the values of the inhibition coefficient do not seem to be influenced by the experimental conditions in the range studied.

The chemical composition of the water strongly influences the efficiency of the disinfection process. However, the effect of different inorganic anions has been found to be produced at very different concentration levels and by different mechanisms, which also affects the values of the kinetic and pseudo-adsorption constants in different ways. Similarly, low concentrations of humic substances inhibit the disinfection process, whereas the same concentration of sucrose does not affect at all. Consequently, the macroscopic analysis of real waters based on conductivity and total organic carbon measurements must be carefully considered, as differences in the nature of the inorganic and organic substances present in similar waters could lead to unexpected results.

Keywords: Photocatalytic disinfection; Kinetics; *Escherichia coli*; Supported TiO_2; Water composition

1. Introduction

During the last years, there has been an increasing public concern related with the use of chlorination processes for the disinfection of drinking water supplies and the formation of potentially harmful chloro-organic disinfection by-products (DBPs) coming from the reaction with naturally-occurring organic matter (NOM) [1–3]. Two of the major classes of DBPs are trihalomethanes (THMs) and haloacetic acids (HAAs), both of which have been shown to present carcinogenic and mutagenic effects on mammals. The most extended commercial alternatives to the use of chlorine-based oxidants are ozonation and short wavelength UV-C irradiation. These processes generally reduce the formation of regulated THMs and HAAs, although, they can increase the levels of other potentially toxicologically important DBPs [1,4].

Among the processes currently in development, semiconductor photocatalysis has emerged as a very attractive, environment-friendly technology for water disinfection, especially considering the possibility of using solar light to drive the process [5]. This process is based on the use of a large band-gap semiconductor material such as TiO_2 to generate the reactive oxygen species (ROS) responsible for the microorganisms inactivation upon irradiation with near ultraviolet radiation. Photocatalytic processes present significant advantages for their application to the disinfection of water resources in rural areas of developing countries in which the access to chemical oxidants is limited but usually high levels of solar irradiation are available during the whole year [6,7]. However, the practical application of photocatalysis for water treatment is usually hindered by difficulties of post-reaction catalyst separation. Consequently, although TiO_2 slurries have been shown to be more active that immobilized systems, many efforts have been devoted to the development of highly active supported photocatalysts [8].

The identification and enumeration of all the possible microorganisms present in a water sample is of impractical

* Corresponding author. Tel.: +34 91 488 7007; fax: +34 91 488 7068.
E-mail address: rafael.vangrieken@urjc.es (R. van Grieken).

0926-3373/$ – see front matter © 2008 Elsevier B.V. All rights reserved.
doi:10.1016/j.apcatb.2008.01.002

application. Consequently, the microbiological assessment of the water quality is usually carried out through the use of indicator microorganisms. *Escherichia coli* constitutes the most widely accepted indicator of the existence of faecal contamination in water, as it is universally present in the intestinal tract of a large number of warm-blooded animals. *E. coli* is a prokaryotic organism consisting on a single autonomous cell, well known from the genetic and physiologic point of view. It belongs to the family *Enterobacteriaceae*, which are defined as Gram-negative, non-sporeforming, rod-shaped and facultative anaerobes, what means that they can have both a respiratory and a fermentative type of metabolism [9].

Since the early work of Matsunaga et al. [10], many research groups have reported the application of semiconductor photocatalysis to the inactivation of different kind of pathogenic microorganisms, such as bacteria, viruses, algae, fungi or protozoa [11]. The bactericidal effects of TiO_2 photocatalysis, and especially the inactivation of *E. coli* suspensions, are by far, the most reported studies [12,13]. Several studies have focused on the study on the effects of operational parameters such as light intensity and titanium dioxide concentration [14,15] and on the use of solar light [16], whereas other works have reported the influence of the chemical composition of water [17,18] and the application of this technology for the disinfection of crude water [19] and wastewaters [20]. However, in most cases the disinfection profiles are described by very simple empirical equations, and only few attempts have been made to describe the kinetics of the photocatalytic disinfection from a mechanistic point of view.

This work is focused on the kinetic analysis of the photocatalytic inactivation of *E. coli* using a model based on a simplified reaction mechanism. We have studied the influence of the concentration of TiO_2 on the kinetics and also of the presence in the water of different inorganic and organic compounds. Finally, the activity of two different TiO_2/SiO_2 photocatalysts has been evaluated and compared with their performance for the photocatalytic oxidation of chemical pollutants.

2. Experimental

2.1. Catalysts

Most of the photocatalytic experiments were carried out by using commercial titanium dioxide (Degussa P25, S_{BET} = 50 $m^2\ g^{-1}$, 80:20 anatase:rutile ratio). TiO_2/SiO_2 materials with a nominal content of 60 wt% of titania were prepared by incorporation of titanium dioxide using a sol–gel method starting from titanium tetraisopropoxide. Two different silica materials were used as support: (i) a commercial silica (INEOS ES70Y, S_{BET} = 257 $m^2\ g^{-1}$, V_P = 1.15 $cm^3\ g^{-1}$) and (ii) a home-made SBA-15 mesostructured silica (S_{BET} = 640 $m^2\ g^{-1}$, V_P = 0.96 $cm^3\ g^{-1}$). In all cases, the catalysts were used in suspension, being the supported TiO_2/SiO_2 materials much easier to recover. More details about the synthesis procedure, characterization and photocatalytic activity of these materials can be found elsewhere [21,22].

2.2. Photocatalytic disinfection experiments

The photoreactor consist of a 1 L cylindrical Pyrex vessel with an opening in the upper part for withdrawal of samples, placed on a rotary shaker. Outer irradiation was used with a UV-A lamp (Radium Suprablack, HBT 125 W) with a very well defined emission peak at 365 nm. The UV-A incident photon flow, determined by ferrioxalate actinometry, was 5.6×10^{-7} einstein $L^{-1}\ s^{-1}$.

E. coli K12 strains (CECT 4624, corresponding to ATCC 23631, where CECT stands for "Colección Española de Cultivos Tipo") were used to prepare the bacterial suspensions. Fresh liquid cultures were prepared by inoculation in a Luria-Bertani nutrient medium (Miller's LB Broth, Scharlab) and incubation at 37 °C for 24 h under constant stirring on a rotary shaker.

To prepare the reaction suspensions, 5 mL of the liquid culture (with a stationary concentration around 10^9 CFU mL^{-1}) were centrifuged to recover the bacteria and resuspended in 5 mL of sterile deionized water (Milli-Q®, 18.2 MΩ cm). The centrifugation and rising sequence was repeated twice. Finally, 1 mL of the aqueous *E. coli* suspension was diluted to 1 L with MilliQ water to achieve an initial concentration of bacteria around 10^6 CFU mL^{-1}.

For experiments in the presence of inorganic materials, sodium salts of chloride, phosphate and hydrogen carbonate were used (Scharlab, reagent grade). Humic acids (Sigma–Aldrich, technical grade) and commercial sucrose were used as organic additives. These compounds, when present, were added to the bacterial suspension together with the catalyst without further pH adjustment. Prior to the beginning of the reaction, this suspension was homogenized in the dark for 30 min under stirring in a rotary shaker at 140 rpm. In the meantime, the lamp was switched on to stabilize its emission power and spectrum before the photocatalytic experiments were started.

The analysis of the samples during the reaction was carried out following a standard serial dilution procedure. Each decimal dilution was spotted eight times on LB nutrient agar plates (Miller's LB Agar, Scharlab) and incubated at 37 °C for 24 h before counting.

3. Results and discussion

3.1. Disinfection kinetics: empirical approach

Fig. 1 shows the results of the photocatalytic inactivation of *E. coli* aqueous suspensions using Degussa P25 TiO_2 with different catalyst loadings. As it can be seen, three different regions can be identified in the plot: (i) an initial delay or smooth decay at the beginning of the reaction, usually called "shoulder", (ii) a log-linear inactivation region that covers most part of the reaction and (iii) a deceleration of the process at the end of the reaction, usually called "tail". Similar profiles have been previously reported in the literature and their physical meaning suggested [15].

Due to the complex mechanism of the disinfection processes, the kinetic analysis of the photocatalytic bacterial

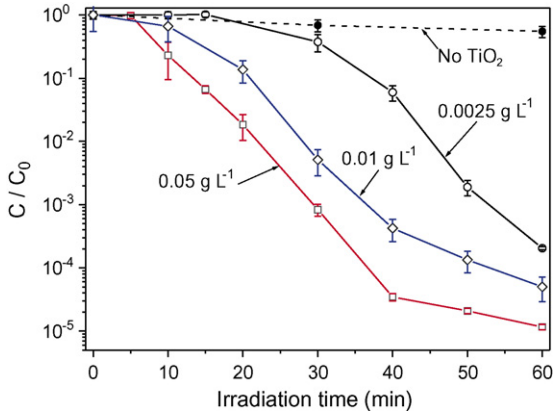

Fig. 1. Photocatalytic inactivation of 10^6 CFU mL^{-1} *E. coli* suspensions with different loadings of Degussa P25 TiO_2 (error bars calculated from eight independent bacteria counting measurements).

inactivation has been usually carried out using empirical equations. The classical disinfection model reported in the literature is the Chick–Watson equation, dating from 1908 [23,24] and whose general expression is given by:

$$\log\left(\frac{C}{C_0}\right) = -k[c]^n t \tag{1}$$

where C/C_0 is the reduction in the bacterial concentration, k is the disinfection kinetic constant, c is the concentration of the disinfecting agent at time t and n the reaction order. In photocatalytic processes with artificial light, the concentration of the disinfecting agent could be considered to be constant with time for a fixed catalyst concentration and photoreactor–lamps configuration. Consequently, in this case the equation could be rewritten as follows:

$$\log\left(\frac{C}{C_0}\right) = -k' t \tag{2}$$

Due to the simplicity of this log-linear equation corresponding to a pseudo-first order kinetics, this model has been widely used in the literature to compare the efficiency of different disinfection processes through the values of the kinetic constant, k'. However, the correct application of the model requires that the disinfection rate does not vary at all during the process. Consequently, this model is only valid for the description of the second region (the log-linear) identified in Fig. 1.

Several authors have assigned the initial delay at the beginning of the reaction to the existence of a lag stage in the inactivation of the bacteria [25,26]. In these cases, the delayed Chick–Watson model should be better used to fit the experimental results. This model includes a second parameter called t_0 that corresponds to the time of delay, according to the expression:

$$\log\frac{C}{C_0} = \begin{cases} 0 & \text{for} \quad t \le t_0 \\ -k'(t - t_0) & \text{for} \quad t > t_0 \end{cases} \tag{3}$$

In other cases, the disinfection rate remains constant from the beginning of the reaction showing a deceleration after a long period of treatment, when the concentration of bacteria is very low. In this case, a modification of the Chick–Watson could be applied [27], according to the following two-parameters expression:

$$\log\frac{C}{C_0} = k_1[1 - \exp(-k_2 t)] \tag{4}$$

This modified Chick–Watson model could reproduce either the existence of a shoulder at the beginning of the reaction or a tail at the end. However, this equation cannot reproduce the simultaneous existence of both regions.

The disinfection model proposed by Hom Eq. (5) dates from 1972 [28] and it can be applied when the bacterial inactivation deviates from the classical log-linear behaviour:

$$\log\left(\frac{C}{C_0}\right) = -k' t^h \tag{5}$$

The expression is very similar to the Chick–Watson model represented in Eq. (1), but incorporating a second parameter called h. For the case $h = 1$, this equation simplifies to the Chick–Watson linear equation; for $h > 1$, the Hom model reproduces the existence of a shoulder at the beginning of the reaction, whereas, for $h < 1$ the equation permits the fitting of a tail at the end of the process. However, once again, this model is unable to reproduce the simultaneous existence of both regions.

Finally, a modification of the original Hom equation has been also proposed [27] that can be simplified to the expression:

$$\log\frac{C}{C_0} = -k_1[1 - \exp(-k_2 t)]^{k_3} \tag{6}$$

when applied to the case of constant concentration of the disinfecting agent that can be assumed in photocatalytic processes. This three-parameter model makes possible the fitting of disinfection profiles with three different regions corresponding to an initial delay, a log-linear disinfection region and a final tail.

Fig. 2 summarizes graphically the features of these disinfection kinetic models. From these graphs it is clear that the modified Hom model is the only one that could be able to reproduce the experimental results reported in Fig. 1. As it can be seen in Fig. 3, the modified Hom model successfully fits the inactivation data. However, the null physical meaning of its parameters makes the comparison difficult among the experiments based on the numerical values. From a structural point of view, an equation with at least three parameters is required to successfully fit experimental data with both a shoulder and a non-symmetrical tail. Consequently, it would be desirable to find a kinetic model with a mechanistic base that gives physical meaning to its parameters.

3.2. Disinfection kinetics: mechanistic approach

Up to here, we have presented the kinetic models usually applied to fit the experimental data obtained in the disinfection of water using advanced oxidation processes based on the formation of species with a high oxidation potential, such as

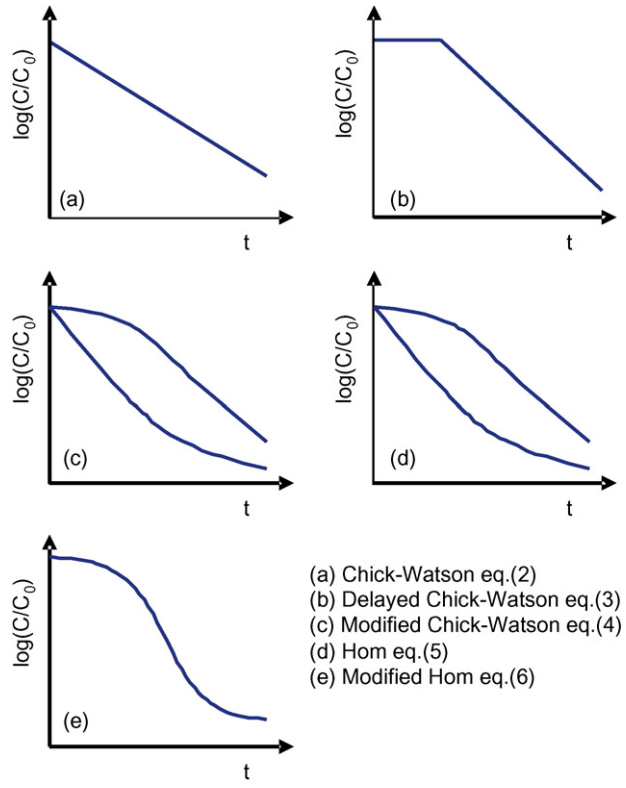

Fig. 2. Graphical shape of several kinetic models commonly used in photocatalytic disinfection studies.

hydroxyl radicals, generated upon addition of chemical oxidants such as ozone or hydrogen peroxide, in the presence or not of a photon source and a suitable semiconductor material. However, the kinetic modelling of disinfection processes has been studied in depth in other scientific and technological areas. For instance, Geeraerd et al. [29] reported an extended review of a large number of microbial inactivation models used in the food industry for the sterilization of cooked products using a mild thermal treatment. Their work derived in the development

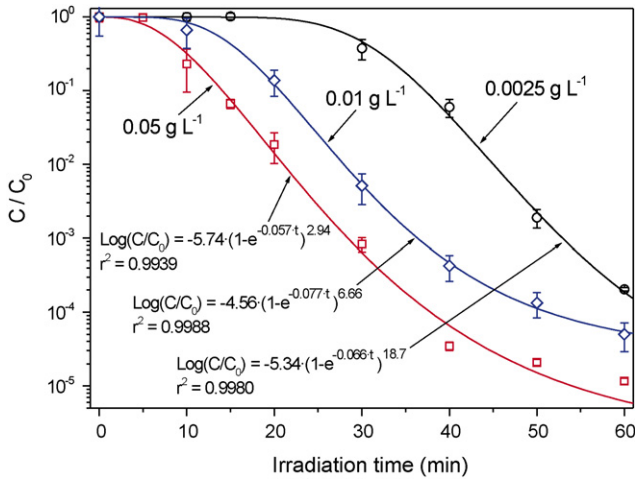

Fig. 3. Fitting of the modified Hom kinetic model to experimental data of the photocatalytic inactivation of 10^6 CFU mL^{-1} *E. coli* suspensions with different loadings of Degussa P25 TiO_2 (error bars calculated from eight independent bacteria counting measurements).

of a user-friendly Microsoft® Excel tool called GInaFIT [30] provided for end-users in the food industry not familiar with non-linear regression analysis tools. GInaFiT covers all known survivor curve shapes for vegetative bacterial cells including classical log-linear curves, with and without shoulders and/or tails, concave and convexes curves, biphasic inactivation kinetics, etc. This tool is a recommended way of testing models with different shapes to easily describe the deactivation kinetics for food sterilization. However, the significant differences in the fundamentals of the thermal sterilization of food and water disinfection using heterogeneous photocatalysis or other advanced oxidation technologies makes necessary a different mechanistic approach for the modelling of the bacterial inactivation in water.

The presence of the shoulder can be justified by a single-hit multiple-target or a series event phenomenon in which the damage to the cell is cumulative rather than instantly lethal. This concept has been applied to the description of bacterial thermal inactivation [29] and also to the bacterial inactivation under high energy UV-C irradiation [31,32]. In the first case, a large number of critical molecules need to be denatured before of the cell inactivation. In the second one, as UV-C photons are absorbed by DNA, an important genetic damage must be produced to hinder the bacteria reproduction.

The reaction scheme of the series event bacterial inactivation model first proposed by Severin et al. [31] could be represented as follows:

$$C_0 \xrightarrow{k_1} C_1 \xrightarrow{k_2} \cdots C_i \xrightarrow{k_i} \cdots C_{n-1} \xrightarrow{k_n} C_n \tag{7}$$

where C_i ($i = 0, 1, 2, \ldots, i, \ldots, n$) represents the population of bacteria with a damage level i, k_i is the kinetic constant between the damage level $i-1$ to the damage level i and n is the threshold limit of damage that produce the bacterial inactivation. According to Eq. (7), $n+1$ differential equations would be required to accurately describe the process. However, assuming that all the kinetic constants are equal ($k_1 = k_2 = \cdots k_i \cdots = k_n = k$), the evolution of the active bacterial population could be calculated by the following expression [14]:

$$\log \frac{C}{C_0} = \log \frac{\sum_{i=0}^{n-1} C_i}{C_0} = -kt + \ln\left(1 + \sum_{i=1}^{n} \frac{(kt)^i}{i!}\right) \tag{8}$$

According to the photocatalytic disinfection mechanism proposed by Sunada et al. [33], the ROS generated upon irradiation of the semiconductor particles causes the bacterial inactivation by producing the partial decomposition of the external membrane, changing its permeability or destroying it, allowing the ROS to reach the cell wall and the cytoplasmic membrane, leading to the lysis of the cell. Consequently, bacteria are inactivated as a consequence of the cumulative effects of serial ROS attacks on the cell membrane-wall system.

The length of the shoulder region in the inactivation curves would depend on the volumetric rate of ROS generation, conditioned by the concentration of the semiconductor in the aqueous suspension and by the incident radiation flow, both factors determining the volumetric rate of photon absorption.

Consequently, higher values of the volumetric rate of photon absorption not only increase the slope of the log-linear deactivation region, but also make the length of the initial shoulder shorter. This effect can be clearly observed in Fig. 1.

The length of the shoulder region would also depend on the average number or ROS attacks required for the inactivation of one single cell. This value should be different depending on the specific organism and in a real microbial population could show a distribution of frequencies, as not all the individuals would show the same resistance. For instance, the maximum disinfection rate from the experiment using 0.05 g L^{-1} TiO_2 represented in Fig. 1 is around 3×10^6 CFU L^{-1} s^{-1}. Dividing this value per the number of photons arriving at the reactor determined by ferrioxalate actinometry (3.4×10^{17} photo-photons L^{-1} s^{-1}), an apparent photonic efficiency in the order of 10^{-11} CFU $photon^{-1}$ is calculated. The comparison of this number with the quantum yield of 0.04 for hydroxyl radical generation reported by Sun and Bolton [34] shows that the number of hydroxyl radicals required for the inactivation of a single *E. coli* bacterium is in the order of 10^9. Similar results can be calculated from the experimental data reported by Cho et al. [26] dealing with the correlation between the inactivation of *E. coli* and the concentration of hydroxyl radicals.

From the previous calculations, it can be derived that the accurate description of the photocatalytic inactivation of bacteria using the series event model Eq. (8), would required a very large number of damage levels that makes unfeasible its application from a practical point of view.

Concerning the tail at the end of the inactivation profiles, Geeraerd et al. [29] reported several vitalistic and mechanistic explanations for the presence of a microbial subpopulation resistant to the thermal sterilization of food (C_{res}). This subpopulation would be genetically more resistant, adapted or inaccessible to the heat. Similar considerations have been claimed by Najm [35] to explain the presence of the shoulders and/or tails as a consequence of intrinsic distribution of bacterial resistance to the disinfecting agent. Most of these explanations are plausible for the food processing due to the genetic heterogeneity of the microorganisms and the temperature profiles inside the food. However, they are not able to explain the tailing phenomenon in the water disinfection treatment represented in Fig. 1 in which well-mixed conditions assures that all the bacteria should receive the same lethal dose, and being a genetically cloned bacterial population (theoretically all the individuals would be equally resistant to the process as they derived from the same culture). Another possibility is that the resistance is developed during the treatment, as suggested by Berney et al. [36] for thermal, UVA and solar disinfection. However, as shown by Rincon and Pulgarín [37], the repair mechanisms responsible of that resistance are not so important when TiO_2 is present in the suspension. Consequently, the concept of a subpopulation resistant to the treatment seems to be not really applicable to the water photocatalytic disinfection. Moreover, this C_{res} value imposes an asymptotic limit to the inactivation process, which means that total disinfection is not possible. In contrast, the results represented in Fig. 1 seem to indicate that the rate of the inactivation process decreases at the end of the reaction but a total disinfection would be possible after sufficient time. For this reason, the tail seems to be more related to an inhibition phenomenon produced by the competition of the organic products released to the medium rather than to an intrinsic resistance of the bacteria, as suggested by Benabbou et al. [15].

Taking into account all the considerations mentioned above, we propose the following scheme for the photocatalytic bacterial inactivation:

$$C_{undam} \xrightarrow{k_1} C_{dam} \xrightarrow{k_2} C_{inact} \xrightarrow{k_3} C_{prod} \tag{9}$$

where C_{undam} represents the undamaged population of bacteria, C_{dam} is a lump of the bacteria in all the intermediate levels of damage, C_{inact} is the population of inactivated bacteria and C_{prod} are the subsequent products of degradation formed from the oxidation of the organic components released to the medium after the bacterial lysis (also expressed as equivalent bacterial population).

The usual measurement in the disinfection experiments is the concentration of viable bacteria, i.e. $C_{undam} + C_{dam}$, due to the difficulties of the identification and quantification of the inactivated bacteria and the lysis and oxidation products, C_{inact} and C_{prod}, respectively. Considering that a bacteria-catalyst interaction is required for the reaction to take place, we propose the use of Langmuir–Hinshelwood-like kinetic equation for the description of the reaction rate in the mass balance of the two species of interest:

$$\frac{dC_{undam}}{dt} = \frac{-k_1 K_{undam} C_{undam}^{n_{undam}}}{1 + K_{undam} C_{undam}^{n_{undam}} + K_{dam} C_{dam}^{n_{dam}}} \tag{10}$$

$$\frac{dC_{dam}}{dt} = \frac{k_1 K_{undam} C_{undam}^{n_{undam}} - k_2 K_{dam} C_{dam}^{n_{dam}}}{1 + K_{undam} C_{undam}^{n_{undam}} + K_{dam} C_{dam}^{n_{dam}}} \tag{11}$$

where three different kind of parameters have been considered:

(i) Kinetic constants, k_i, representing the rate of the reaction of ROS with bacteria. These constants are the unique parameters considered when applied the log-linear Chick–Watson model.

(ii) Pseudo-adsorption constants, K_i, which represent the interaction between the catalyst and the bacteria. This constant could be considered similar to the adsorption equilibrium constant that appears in the Langmuir–Hinshelwood heterogenous kinetic model. However, as the size of the microorganisms is larger than that of the titania agglomerates [38], these constants do not represent strictly an adsorption phenomenom but a more general interaction. The introduction of this parameter allows the modelling of kinetic data showing a shoulder at the beginning of the reaction.

(iii) Inhibition coefficients, n_i, accounting for the inhibition produced by the increasing concentrations in the medium of the lysis and oxidation products strongly competing for the ROS. This effect is especially important at the end of the reaction, where high concentrations of these compounds and a small amount of viable bacteria are present in

the suspension. However, due to difficulties related to the identification and quantification of the large amount of released macromolecules, kinetics models based on C_{inact} and C_{prod} are impractical. Instead, we have introduced an inhibition coefficient that essentially means that the reaction order with respect to the bacteria concentration is higher than one. This approach has been previously used in enzymology for the description of the reaction rate of complex systems such as cooperative enzymes, allosteric control and inhibition by product through the Hill equation and the so-called Hill coefficient [39]. The introduction of these constants in the kinetic model permits the fitting of experimental data showing a tail at the end of the reaction.

One of the disadvantages of the kinetic model represented by Eqs. (10) and (11) is that six independent parameters are required to describe the reaction rate. Consequently, there is a high risk of overfitting the experimental data, and, moreover, the statistical significance of the parameters and the plausibility of the model will be very low. Taking into account that the intrinsic kinetics of the ROS attack, the TiO_2–bacteria interaction and the inhibition by products should be similar for both undamaged and damaged bacteria, we can assume that:

$$k_1 = k_2 = k \tag{12}$$

$$K_{undam} = K_{dam} = K \tag{13}$$

$$n_{undam} = n_{dam} = n \tag{14}$$

leading to the expressions:

$$\frac{dC_{undam}}{dt} = -k\frac{KC_{undam}^n}{1 + KC_{undam}^n + KC_{dam}^n} \tag{15}$$

$$\frac{dC_{dam}}{dt} = k\frac{KC_{undam}^n - KC_{dam}^n}{1 + KC_{undam}^n + KC_{dam}^n} \tag{16}$$

It must be noticed that the kinetic model represented by Eqs. (15) and (16) requires three independent parameters that can be estimated from the fitting of experimental data. As it has been mentioned above, this is the number of parameters of empirical kinetic models such as the modified Hom equation commonly used to fit survival curves showing, simultaneously, shoulders and tails. However, in contrast with the null physical meaning of the parameters appearing in the empirical models, the mechanistic base of the kinetic model proposed in Eqs. (15) and (16) gives a substantial meaning to the kinetic (k), interaction (K) and inhibition (n) parameters.

Fitting of the model to the experimental measurements of $(C_{undam} + C_{dam})/C_0$ has been carried out using a non-linear regression algorithm coupled with a fifth-order Runge-Kutta numerical integration procedure. As shown in Fig. 4, a very good fitting of the experimental data is obtained in all the experiments.

3.3. Influence of TiO_2 concentration

Figs. 5–7 show values of the kinetic equation parameters as a function of the titania concentration on the suspension. As it is

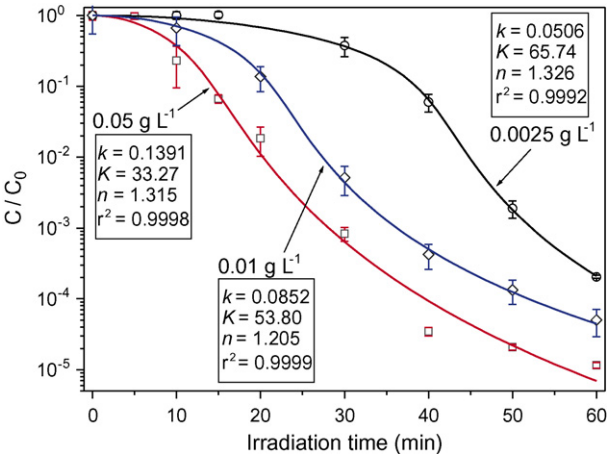

Fig. 4. Fitting of the kinetic model to experimental data of the photocatalytic inactivation of 10^6 CFU mL^{-1} *E. coli* suspensions with different loadings of Degussa P25 TiO_2 (error bars calculated from eight independent bacteria counting measurements). Unit of k: CFU mL^{-1} min^{-1}; unit of K: mL^n CFU^{-n}; n: dimensionless.

shown, the evolution of the kinetic constant follows the classical dependence of the photocatalytic processes. In the lower range of catalyst concentrations, a significant increase in the activity is observed when increasing the amount of TiO_2. These results are explained by the correlation between the bacterial inactivation efficiency and the generation of ROS, as demonstrated Cho et al. [26]. For higher catalyst concentrations, the activity reach a maximum, due to the screening effect of the TiO_2 suspensions that leads to the existence of dark zones at the farthest part of the illuminated reactor volume. Under this regime, the generation of ROS is controlled not by the catalyst concentration, but by the incident radiation flux. Consequently, this critical concentration depends on the irradiation system and the photoreactor geometry, and the value for the present experimental set-up is around 0.05 g L^{-1} of TiO_2.

Similarly, the values of the pseudo-adsorption constant show a marked dependence on the catalysts concentration. A decrease in K is observed as the titania concentration is

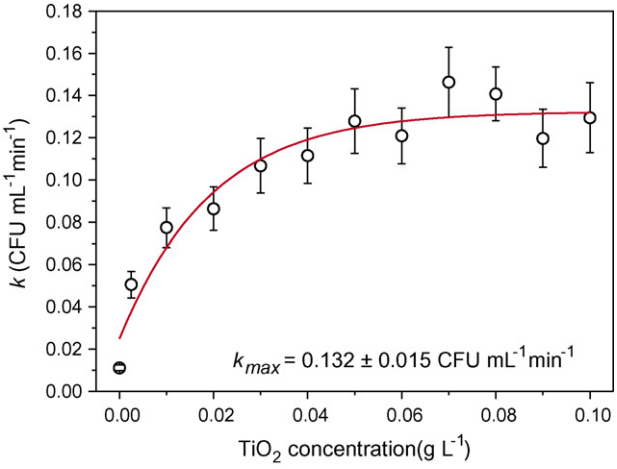

Fig. 5. Influence of Degussa P25 TiO_2 loading on the kinetic constants for the photocatalytic inactivation of 10^6 CFU mL^{-1} *E. coli* suspensions (error bars calculated from two independent experiments).

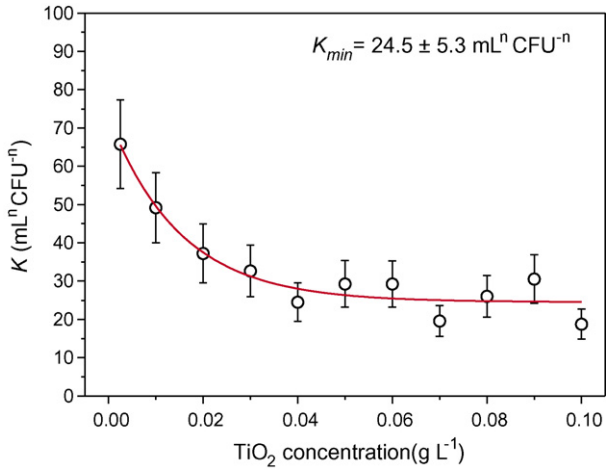

Fig. 6. Influence of Degussa P25 TiO_2 loading on the pseudo-adsorption constants for the photocatalytic inactivation of 10^6 CFU mL^{-1} *E. coli* suspensions (error bars calculated from two independent experiments).

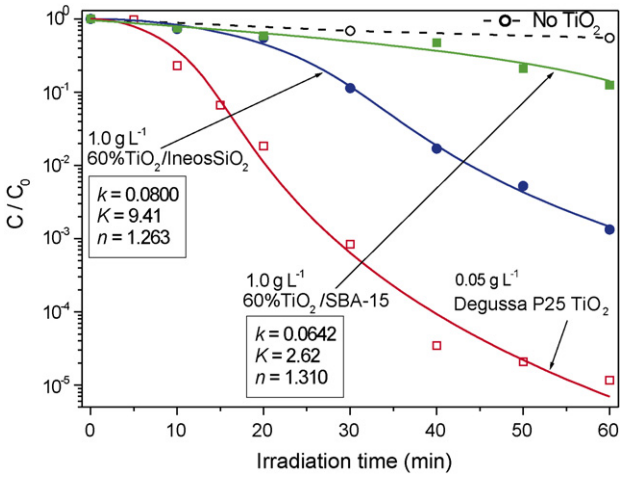

Fig. 8. Photocatalytic inactivation of 10^6 CFU mL^{-1} *E. coli* suspensions with two different silica-supported TiO_2 photocatalysts (error bars have been omitted for clarity purposes). Lines show the fitting of the experimental data with the kinetic model represented by Eqs. (15) and (16). Units of k: CFU mL^{-1} min^{-1}; units of K: mL^n CFU^{-n} ; n: dimensionless.

increased, reaching a asymptotic minimum value of 24.5 ± 5.3 for values higher than 0.05 g L^{-1} of TiO_2 (Fig. 7). As it can be seen, the variation of both parameters seems to be connected; it is confirmed by the high value of the Pearson's correlation coefficients between k and K calculated by the fitting algorithm.

In contrast, the values of the inhibition coefficient do not show a marked dependence on the catalysts concentration, leading to an apparently constant value of 1.31 ± 0.08. Consequently, as predicted in the above discussion, the reaction order of the bacterial concentration is higher than 1, indicating a product inhibition phenomenon that seems to be independent on the catalyst concentration.

3.4. Disinfection with silica-supported TiO_2 photocatalysts

Fig. 8 shows the bacterial inactivation profiles observed when using two different kinds of silica-supported TiO_2 photocatalysts. As it can be seen, the catalysts concentration required to achieve a total absorption of photons is much higher

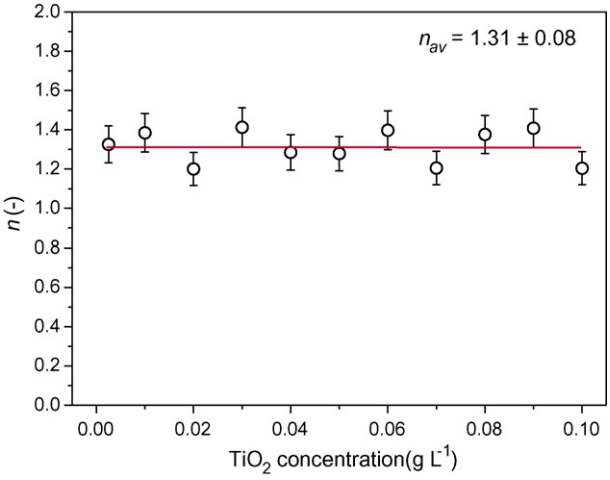

Fig. 7. Influence of Degussa P25 TiO_2 loading on the inhibition coefficient for the photocatalytic inactivation of 10^6 CFU mL^{-1} *E. coli* suspensions (error bars calculated from two independent experiments).

in both cases, due to the much lower absorption coefficients of these materials [22]. The interest for the application of these materials was derived from the high activity previously shown for their use in the photocatalytic oxidation of different cyanide-containing species [40], especially when compared at similar titanium dioxide surface area values [41]. Unfortunately, the activity for bacterial inactivation of both supported photocatalysts is much lower than that of Degussa P25 TiO_2. This low activity leads to a reduction not only in the values of the kinetic constants but also in the pseudo-adsorption parameter. In contrast, both inhibition coefficients are similar to those previously shown for Degussa P25 experiments.

These results derived from the most important difference between the photocatalytic oxidation of chemicals and the inactivation of microorganisms: the size of the target. For powder TiO_2 suspensions, the difference is basically conceptual. Instead of being adsorbed on the titania surface, microorganisms are surrounded by titania particles attached to their external membrane [38]. However, when supported photocatalysts are being used, this difference in size becomes more important. Whereas the molecules can diffuse inside the porous structure of the silica support and reach the titania surface, the contact between titanium and the microorganisms is limited to the TiO_2 crystal located in the external surface of the particles, which represents only an small fraction of the semiconductor loading, especially in the 60% TiO_2/SBA material. Consequently, this kind of material is not suitable for photocatalytic disinfection processes mainly due to the difficulties for the TiO_2–bacteria interaction, that reduce not only the value of the pseudo-adsorption parameter, K, but also the kinetic constant, k.

3.5. Influence of the chemical composition of water

Except for the works of Rincon and Pulgarin [17,18], few works have reported the effect of the chemical composition of

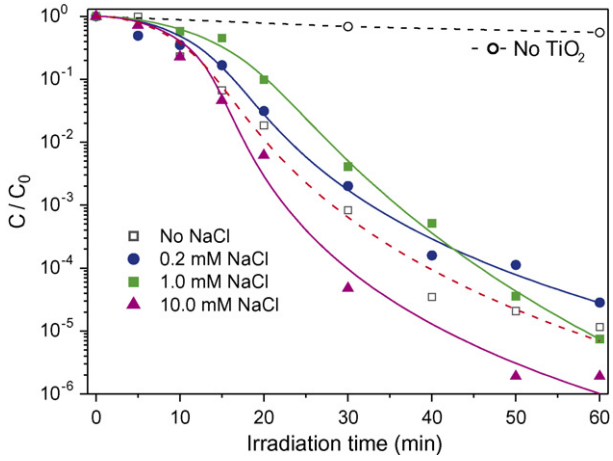

Fig. 9. Influence of the chloride concentration on the photocatalytic inactivation of 10^6 CFU mL^{-1} *E. coli* suspensions with 0.05 g L^{-1} of Degussa P25 TiO_2 (error bars have been omitted for clarity purposes). Lines show the fitting of the experimental data with the kinetic model represented by Eqs. (15) and (16). Units of k: CFU mL^{-1} min^{-1}; units of K: mL^n CFU^{-n} ; n dimensionless.

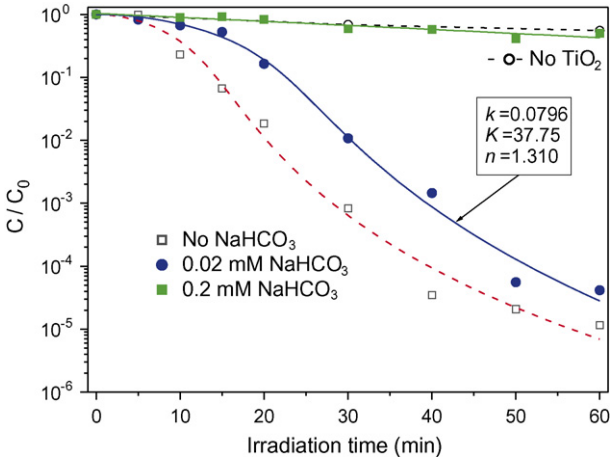

Fig. 10. Influence of the bicarbonate concentration on the photocatalytic inactivation of 10^6 CFU mL^{-1} *E. coli* suspensions with 0.05 g L^{-1} of Degussa P25 TiO_2 (error bars have been omitted for clarity purposes). Lines show the fitting of the experimental data with the kinetic model represented by Eqs. (15) and (16). Units of k: CFU mL^{-1} min^{-1} ; units of K: mL^n CFU^{-n} ; n dimensionless.

water on the efficiency of photocatalytic disinfection processes. This point is crucial for the real application of this technology at field scale, as natural waters usually contain significant concentrations of inorganic ions and organic substances. To investigate the decrease in the activity produced by inorganic anions, experiments with increasing concentrations of chloride, bicarbonate and phosphate were carried out. Fig. 9 shows the inactivation profiles observed in the presence of three different concentrations of sodium chloride in comparison with the reaction performed with deionized water. As it can be seen, low concentrations of chloride do not seem to produce a significant effect on the disinfection efficiency. For higher concentrations of chloride ions, the efficiency is even slightly higher, probably due to the formation of chlorine radicals ($Cl^{\bullet}$) that enhanced the disinfecting activity of the generated ROS.

From a kinetic point of view, Fig. 9 also shows that the mechanistic model represented by Eqs. (15) and (16) fits successfully the experimental data, leading to small differences in the values of the kinetic parameters (essentially on the kinetic constant, k) that correlate the activity observed in the inactivation profiles.

For bicarbonate anions, results are very different, as shown in Fig. 10. Even for very small concentrations such as 0.02 mM, a significant decrease in the inactivation is observed. Moreover, for a concentration of 0.2 mM of $NaHCO_3$ the bacterial survival after 60 min of irradiation is essentially the same than that achieved in the blank experiment without titanium dioxide. From the kinetic modelling point of view, assuming the same inhibition coefficient, the reduction in the activity leads to a decrease in the kinetic constant, the most suitable explanation being the existence of a competition for the ROS between the HCO_3^- anions and the *E. coli* cells. The main difference between the competition produced by the bicarbonate ions and that produced by the organic products derived from the lysis of the cells is that the former does not depend on the irradiation time. Consequently, it affects the kinetic constant, k, and not the inhibition coefficient, n.

The presence of phosphates in the water seems to be even more critical for the disinfection efficiency. As shown in Fig. 11, a total inactivation of the process was observed for 0.02 mM concentrations of Na_3PO_4. In this case, the scavenging of the disinfecting radicals is not enough to justify these results. In addition to that, the decrease in the disinfection rate is probably due to the formation of an inorganic salt layer at the surface of TiO_2, which inhibits the reaction, as suggested by Guillard et al. [42] for the photocatalytic oxidation of methylene blue. This fact could be related with the strong reduction in the value of the pseudo-adsorption parameter in comparison with the mild decrease in the kinetic constant observed for 0.002 mM of Na_3PO_4.

To study the influence of organic compounds, several experiments in the presence of increasing concentration of humic acids were carried out. Humic substances, derived from the decomposition of the organic matter, are the most common

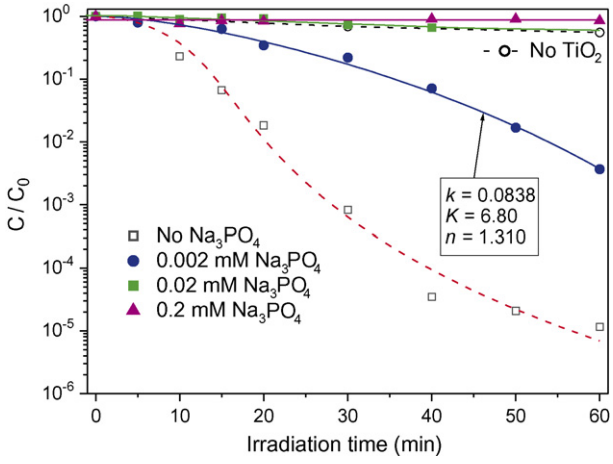

Fig. 11. Influence of the phosphate concentration on the photocatalytic inactivation of 0^6 CFU mL^{-1} *E. coli* suspensions with 0.05 g L^{-1} of Degussa P25 TiO_2 (error bars have been omitted for clarity purposes). Lines show the fitting of the experimental data with the kinetic model represented by Eqs. (15) and (16). Units of k: CFU mL^{-1} min^{-1} ; units of K: mL^n CFU^{-n} ; n dimensionless.

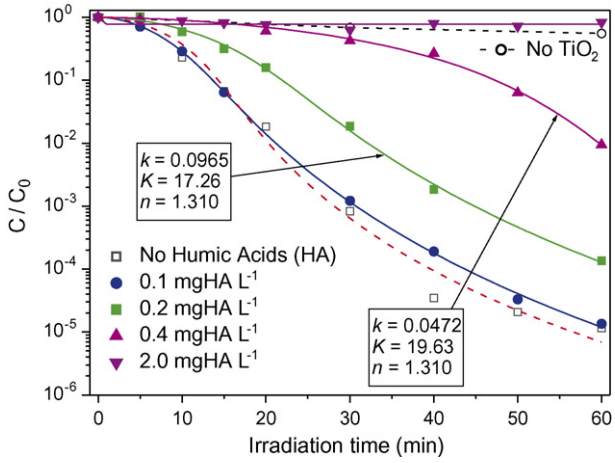

Fig. 12. Influence of the humic acids concentration on the photocatalytic inactivation of 10^6 CFU mL^{-1} *E. coli* suspensions with 0.05 g L^{-1} of Degussa P25 TiO_2 (error bars have been omitted for clarity purposes). Lines show the fitting of the experimental data with the kinetic model represented by Eqs. (15) and (16). Units of k: CFU mL^{-1} min^{-1} ; units of K: mL^n CFU^{-n} ; n dimensionless.

organic compounds present in natural waters. The results reported in Fig. 12 show that for a concentration of 2.0 mg L^{-1} the inhibition of the bacterial inactivation is complete. At lower concentration of humic acids and according to the fitting parameters of the kinetic model, the decrease in the activity seems to be produced by a strong reduction in the kinetic constant together with a slight decrease in the pseudo-adsorption parameter.

The most suitable explanation for this inhibition would be the competition of the organic matter for the oxidizing species. However, experiments in the presence of comparable concentrations of sucrose do not show a reduction in the disinfection rate. This indicates that the inhibition phenomenon is not general, but specific for the humic acids (at least in comparison with carbohydrates). The polyaromatic nature of the humic substances seems to be the factor determining this behaviour, producing a competition for the absorption of UV photons and reducing the amount of radiation available for the semiconductor. Consequently, the nature of the organic matter also seems to be very important for the efficiency of the process.

Finally, an experiment performed in the presence of a complex organic/inorganic mixture (0.2 mM NaCl, 0.02 mM $NaHCO_3$, 0.002 mM Na_3PO_4, 0.2 mg L^{-1} of humic acids) demonstrated that the inhibiting effects are additive, leading to a disinfection activity much lower than that observed in the presence of each constituent individually: k = 0.0415 CFU mL^{-1} min^{-1}, K = 34.70 mL^n CFU^{-n}, and n = 1.31.

4. Conclusions

The photocatalytic inactivation of *E. coli* suspensions has been successfully modelled with kinetic equations based on a simplified reaction mechanism using three parameters: kinetic constant (k), pseudo-adsorption constant (K) and inhibition coefficient (n). In comparison with the empirical equations traditionally used to describe the bacterial inactivation profiles in photocatalytic processes, the parameters of the developed model show physical meaning, which makes the interpretation of the results and the evaluation of the influence of the different process variables easier, especially when complex non log-linear profiles are observed.

The developed model has been used to fit a large number of experiments, and especially those focused on the evaluation of the influence of the titanium dioxide concentration, the chemical composition of water and the activity of silica-supported titanium dioxide photocatalysts. The dependence of k and K with the concentration of TiO_2 is especially interesting for optimizing this operational variable. In contrast, the values of the inhibition coefficients do not seem to be directly influenced by the experimental conditions.

Concerning the application of porous TiO_2/SiO_2 photocatalysts, the main conclusion is that these materials are very inefficient due to restrictions in the access of the bacteria to the TiO_2 surface, leading to reduced values of the kinetic and pseudo-adsorption constants. Consequently, the desirable immobilization of TiO_2 required to improve the separation of the catalyst should be investigated using different approaches.

Finally, the chemical composition of the water has been shown to produce a strong influence on the efficiency of the disinfection process. However, the effect of different inorganic anions has been proved to be produced at very different concentration levels and by different mechanisms, which also affects the values of the kinetic and pseudo-adsorption constants in different ways. Similarly, whereas low concentrations of humic substances inhibit the disinfection process, comparable concentrations of carbohydrates does not affect at all. Consequently, the macroscopic analysis of real waters based on conductivity and total organic carbon measurements must be carefully considered, as differences in the nature of the inorganic and organic substances present in similar waters could lead to unexpected results.

Acknowledgements

The authors gratefully acknowledge the financial support of the Ministerio de Educación y Ciencia of Spain through the program Consolider-Ingenio 2010 (project CSD2006-00044 TRAGUA) and Comunidad de Madrid through the program REMTAVARES S-0505/AMB/0395.

References

[1] S.D. Richardson, Trac-Trends Anal. Chem. 22 (2003) 666–684.
[2] R. Sadiq, M.J. Rodriguez, Sci. Total Environ. 321 (2004) 21–46.
[3] K. Gopal, S.S. Tripathy, J.L. Bersillon, S.P. Dubey, J. Hazard. Mater. 140 (2007) 1–6.
[4] W. Liu, L.-M. Cheung, X. Yang, C. Shang, Water Res. 40 (2006) 2033–2043.
[5] I. Muñoz, J. Rieradevall, F. Torrades, J. Peral, X. Domènech, Sol. Energy 79 (2005) 369–375.
[6] E.F. Duffy, F. Al Touati, S.C. Kehoe, O.A. McLoughlin, L.W. Gill, W. Gernjak, I. Oller, M.I. Maldonado, S. Malato, J. Cassidy, R.H. Reed, K.G. McGuigan, Sol. Energy 77 (2004) 649–655.

[7] S. Gelover, L.A. Gómez, K. Reyes, M.T. Leal, Water Res. 40 (2006) 3274–3280.
[8] J. Marugán, D. Hufschmidt, G. Sagawe, V. Selzer, D. Bahnemann, Water Res. 40 (2006) 833–839.
[9] H.G. Schegel, General Microbiology, Cambridge University Press, Cambridge, 1992.
[10] T. Matsunaga, R. Tomoda, T. Nakajima, H. Wake, FEMS Microbiol. Lett. 29 (1985) 211–214.
[11] C. McCullagh, J.M.C. Robertson, D.W. Bahnemann, P.K.J. Robertson, Res. Chem. Intermed. 33 (2007) 359–375.
[12] P.S.M. Dunlop, J.A. Byrne, N. Manga, B.R. Eggins, J. Photochem. Photobiol. A: Chem. 148 (2002) 355–363.
[13] H.M. Coleman, C.P. Marquis, J.A. Scott, C.-C. Chin, R. Amal, Chem. Eng. J. 113 (2005) 55–63.
[14] Y. Horie, D.A. David, M. Taya, S. Tone, Ind. Eng. Chem. Res. 35 (1996) 3920–3926.
[15] A.K. Benabbou, Z. Derrriche, C. Felix, P. Lejeune, C. Guillard, Appl. Catal. B: Environ. 76 (2007) 257–263.
[16] P. Fernández, J. Blanco, C. Sichel, S. Malato, Catal. Today 101 (2005) 345–352.
[17] A.G. Rincón, C. Pulgarín, Appl. Catal. B: Environ. 51 (2004) 283–302.
[18] A.G. Rincón, C. Pulgarín, J. Sol. Energy Eng. 129 (2007) 100–110.
[19] J. Wist, J. Sanabria, C. Dierolf, W. Torres, C. Pulgarín, J. Photochem. Photobiol. A: Chem. 147 (2002) 241–246.
[20] J.A. Herrera Melián, J.M. Doña Rodriguez, A. Viera Suárez, E. Tello Rendón, C. Valdés do Campo, J. Araña, J. Pérez Peña, Chemosphere 41 (2000) 323–327.
[21] R. van Grieken, J. Aguado, M.J. López-Muñoz, J. Marugán, J. Photochem. Photobiol. A: Chem. 148 (2002) 315–322.
[22] J. Marugán, R. van Grieken, O.M. Alfano, A.E. Cassano, AIChE J. 52 (2006) 2832–2843.
[23] H. Chick, J. Hyg. 8 (1908) 92–158.
[24] H.E. Watson, J. Hyg. 8 (1908) 536–542.
[25] J.L. Rennecker, B.J. Mariñas, J.H. Owens, E. Rice, Water Res. 33 (1999) 2481–2488.
[26] M. Cho, H. Chung, W. Choi, J. Yoon, Water Res. 38 (2004) 1069–1077.
[27] M. Cho, H. Chung, J. Yoon, Appl. Environ. Microbiol. 69 (2003) 2284–2291.
[28] L.W. Hom, J. Sanitary Eng. Div. 98 (1972) 183–194.
[29] A.H. Geeraerd, C.H. Herremans, J.F. Van Impe, Int. J. Food Microbiol. 59 (2000) 185–209.
[30] A.H. Geeraerd, V.P. Valdramidis, J.F. Van Impe, Int. J. Food Microbiol. 102 (2005) 95–105.
[31] B. Severin, M. Suidan, R. Engelbrecht, Water Res. 17 (1983) 1669–1678.
[32] M.D. Labas, C.A. Martín, A.E. Cassano, Chem. Eng. J. 114 (2005) 87–97.
[33] K. Sunada, T. Watanabe, K. Hashimoto, J. Photochem. Photobiol. A: Chem. 156 (2003) 227–233.
[34] L. Sun, J.R. Bolton, J. Phys. Chem. 100 (1996) 4127–4134.
[35] I. Najm, J. Am. Water Works Assoc. 98 (2006) 93–101.
[36] M. Berney, H.-U. Weilenmann, J. Ihssen, C. Bassin, T. Egli, Appl. Environ. Microbiol. 72 (2006) 2586–2593.
[37] A.G. Rincón, C. Pulgarín, Appl. Catal. B: Environ. 49 (2004) 99–112.
[38] J. Blanco-Gálvez, P. Fernández-Ibáñez, S. Malato-Rodríguez, J. Sol. Energy Eng. 129 (2007) 4–15.
[39] A. Cornish-Bowden, Fundamentals of Enzyme Kinetics, Portland Press, London, 1995.
[40] M.J. López-Muñoz, R. van Grieken, J. Aguado, J. Marugán, Catal. Today 101 (2005) 307–314.
[41] J. Marugán, M.J. López-Muñoz, J. Aguado, R. van Grieken, Catal. Today 124 (2007) 103–109.
[42] C. Guillard, E. Puzenat, H. Lachheb, A. Houas, J.-M. Herrmann, Int. J. Photoenergy 7 (2005) 1–9.